Application of Parabolic Equation Methods to HF Propagation in an Arctic Environment

Alan D. Thomson and Tan D. Quach

Abstract—**This paper demonstrates the usefulness and flexibility of parabolic equation methods when applied to high frequency (HF) propagation calculations over cliffs and in realistic arctic environments, which are required for estimating the performance of High Frequency Surface Wave Radar (HFSWR). All calculations are performed using a modified version of the TERPEM (TERrain Parabolic Equation Model) software package. This software has been tested extensively through comparisons with other models. As an example, a comparison between data generated with TERPEM and data published in the literature is shown. Calculations performed for four cliff heights (0, 102, 300, 498 m) show that the cliff does not significantly affect the propagation of HFSWR signals at the ranges of interest. Site-specific calculations performed for realistic arctic conditions (cold, low-salinity water covered with broken sea ice and snow) show that HFSWR propagation can be equal to or better than that for ice-free conditions over a significant range for a significant portion of the year (~3 or 4 months). Based on these results, and other considerations related to sea clutter, ionospheric clutter, and man-made noise, it is concluded that useful operation of HFSWR at specific sites in the arctic should be feasible for a significant portion of the year.**

Index Terms—**Arctic regions, high frequency (HF) radar, propagation, sea ice, snow, surface waves.**

I. Introduction

HIGH FREQUENCY Surface Wave Radar (HFSWR) is an effective and relatively low-cost means of providing over-the-horizon surveillance of surface vessels and low-flying aircraft in coastal regions. For example, off the east coast of Newfoundland, these radars have demonstrated the capability to detect and track surface vessels over the full range of the exclusive economic zone (Chan [1]). However, it is not clear whether these HFSWR systems can be used effectively in the Arctic.

The Arctic presents a different operating environment than that of the ocean, for example, along the east coast of Newfoundland. In particular, arctic waters are colder, have lower salinity, and may be covered or partially covered with sea ice. Such conditions will greatly affect the propagation of the HFSWR signals, but not necessarily in a negative way.

Investigations of HF propagation over sea ice (e.g., Hill and Wait [2]), and over mixed land, sea, and sea-ice paths (e.g., Hill and Wait [3]), have been performed using, for example, a "residue series" approach. While these calculations have demonstrated the physical effects associated with propagation over ice-covered seas and over transitions from one of the terrain types to the next, they were limited to two-segment paths. The variation in sea-ice properties over the long ranges associated with HFSWR requires many terrain segments to be considered if an evaluation is to be made of the HFSWR propagation at a specific arctic site. Site-specific calculations incorporating realistic sea-ice variations are also required if the modeled predictions are to be compared with experimental measurements.

To investigate HFSWR propagation in the Arctic (see Thomson and Quach [4]), Defence Research and Development Canada—Ottawa (DRDC Ottawa) funded the modification (Levy and Craig [5]) of the commercial software package TERPEM (TERrain Parabolic Equation Model, [6], Signal Science Ltd.) to allow for calculations to be performed over multilayer ground (Wait [7, p. 10]; see also Hill and Wait [2]), such as an ice-covered sea, using HF antennas located on the ground. The flexibility of the parabolic equation methods (Levy [8]) used in TERPEM allows a large number of terrain segments to be considered. In addition, TERPEM can also consider variation of the terrain elevation, which enables the modeling of antennas located on cliffs. This is an important capability since in many cases, due to land availability and broadcast restrictions, it may be easier or cheaper to locate an HFSWR system on a cliff.

This paper demonstrates the usefulness and flexibility of using parabolic equation methods (TERPEM) for HF propagation calculations over cliffs, and also, in combination with the multilayer ground formulation given by Wait [7, p. 10] (see also Hill and Wait [2]), for HF propagation calculations in realistic arctic conditions (e.g., broken sea ice, snow). In addition, the calculated results allow an assessment of the feasibility of operating HFSWR systems in Canada's Arctic and on cliffs.

II. Propagation Factor

The main output provided by the TERPEM software is the pattern propagation factor (see Blake [9, pp. 8–12]), which is defined as the ratio of the electric field that actually impinges on the target to the electric field that would exist at the target under free-space conditions with the antenna positioned such that the target is in the maximum-gain direction of the antenna pattern. TERPEM calculates the pattern propagation factor by numerically solving an approximation to Maxwell's equations (see Levy [8]). This factor accounts for the effects of diffraction, refraction, reflection, absorption by atmospheric gases, and the gain pattern of the antenna. In addition, this factor includes the "ground-wave attenuation factor" (see Jordan and Balmain [10, p. 645]). The power that would be received by a HFSWR is directly proportional to the 1-way pattern propagation factor F_T^2, which represents the propagation of the radar signals from the

Manuscript received March 11, 2004; revised May 25, 2004.

The authors are with Defence Research and Development Canada—Ottawa, Ottawa, ON K1A 0Z4, Canada (e-mail: Alan.Thomson@drdc-rddc.gc.ca).

Digital Object Identifier 10.1109/TAP.2004.838751

transmit antenna to the target of interest, and to the 1-way propagation factor F_R^2, which represents the propagation of the signals backscattered from the target to the receive antenna. Consequently, the propagation factor has a direct impact on the ability of the HFSWR to detect targets.

III. TERPEM Modifications and Testing

Several modifications made to the TERPEM software (Levy and Craig [5]) are of particular importance for the work presented here. These are the extension of TERPEM's lower frequency limit from 30 to 1 MHz, the modeling of antennas located on or near (in terms of wavelengths) the ground, the modeling of multilayer ground, the increase in the number of grid points available for calculations to one million, and the addition of a wide-angle algorithm. The wide-angle algorithm is mainly required for calculations of propagation over cliffs.

As stated above, the multilayer ground model implemented in TERPEM is taken from Wait [7, p. 10] (see also Hill and Wait [2]). This model represents a structure of differing dielectric layers with a single effective surface impedance. The effective impedance is a function of the frequency, polarization, grazing angle, and the layered structure of the ground. Hill and Wait [2] state that this model of effective surface impedance only requires the assumption that the layers behave locally as a planar structure. In the case of sea-ice, however, the structure is likely to not be exactly horizontally homogeneous. This would result in some form of anomalous propagation within the sea-ice layer that cannot be accounted for by TERPEM when using this effective surface impedance model. Therefore, to be prudent, the use of this model is limited to cases in which the wavelength of the propagating energy is large compared to the thickness of the sea-ice layer.

To test the implementation of the multilayer ground model, TERPEM was used to reproduce most of the calculations of HF propagation over sea-ice performed by Hill and Wait [3]. In general, the comparisons showed very good agreement. Fig. 1 shows an example comparison for the case of Hill and Wait's Fig. 8 [3], where the Hill and Wait data have been extracted from the figures presented in their paper. This example corresponds to the case of a short-dipole vertically polarized antenna transmitting a frequency of 10 MHz. The antenna source point is located 0 m above the sea (relative permittivity, $\varepsilon_r = 80$; conductivity, $\sigma = 1$ S m^{-1}) or ice surface. Ice-covered seas begin at 3 km range. Four different thickness values (0, 25, 50, 100 cm) of sea ice ($\varepsilon_r = 6$; $\sigma = 3.34 \times 10^{-4}$ S m^{-1}) are considered. The data plotted in Fig. 1 correspond to a propagation path spanning from 0 to 100 km range at an altitude of 0 m above the sea or ice surface (see Fig. 2). In each case, the TERPEM results agree well with those of Hill and Wait [3].

Fig. 1 also demonstrates that the TERPEM results include the "recovery effect" and the "interference" effect caused by the presence of the ice layer (see Hill and Wait [2], [3]). The "recovery effect" is the increase in propagation factor observed when the propagating energy moves from the sea to the ice-covered sea region. It is caused by the excitation of a trapped surface wave resulting from the highly inductive surface impedance created by the presence of the ice layer. Interference between the trapped surface wave and ground wave modes occurs at ranges where the magnitudes of the modes are similar, e.g., beginning at ~8 km in Fig. 1 for the case of 50 cm ice thickness.

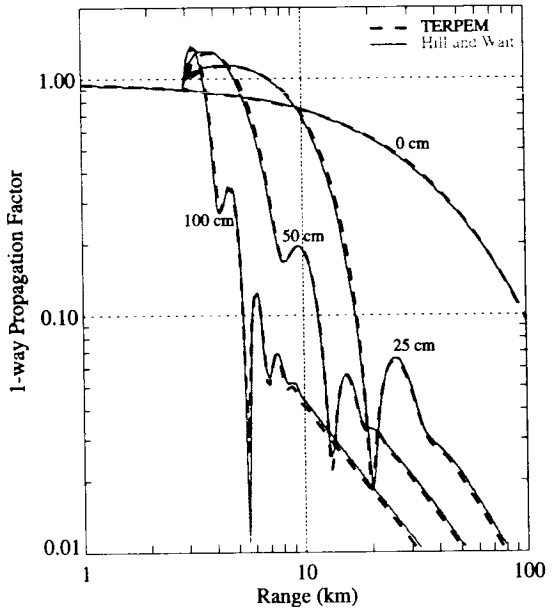

Fig. 1. Comparison of TERPEM calculations with those of Hill and Wait [3, Fig. 8].

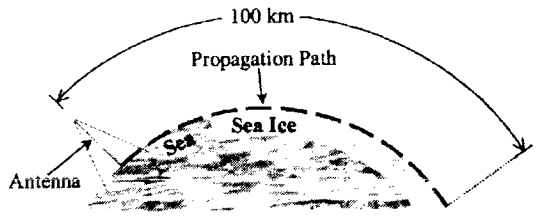

Fig. 2. Geometry for propagation calculations at 0 m altitude over a mixed sea and ice-covered sea path.

IV. Propagation Over Cliffs

To avoid attenuation of the HFSWR signals by the ground, it is best to locate the antennas as close as possible to the sea. When the system is located on a cliff, it is best to locate it as close as possible to the cliff edge. For the calculations presented in this section, the antenna is located at 100 m, or one wavelength, behind the cliff edge.

This geometry can be challenging for TERPEM when using higher frequencies (e.g., X band) for which it has difficulty representing large propagation angles, such as those resulting from the diffraction at the cliff edge. This can lead to inaccurate propagation factor values down range. However, this is not a problem for frequencies in the HF band (e.g., 3 MHz).

The geometry corresponding to the HF cliff calculations is shown in Fig. 3. A 9 m vertical centre-fed linear antenna (see Jackson [11]) is modeled. Thus, the antenna source point is 0 m above a medium dry ground ($\sigma = 0.001$ S m^{-1}, $\varepsilon_r = 15$, at 3 MHz) surface. Propagation factor values are calculated for four different cliff heights (0, 102, 300, 498 m) out to a range of 100 km along a propagation path that is 6 m above the sea surface. The terrain height remains at the cliff height for the first 100

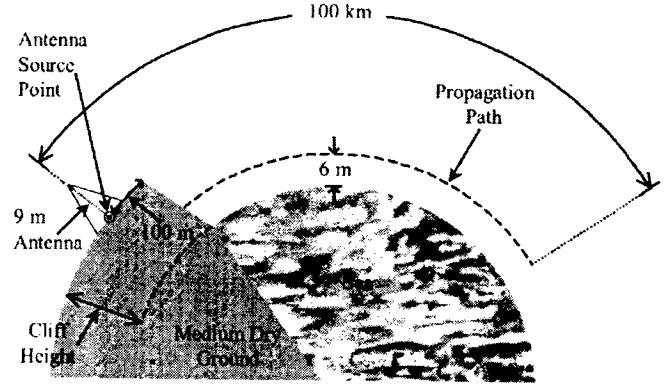

Fig. 3. Geometry for propagation calculations over a cliff. The propagation path is 6 m above the sea, and the antenna is located 100 m behind the cliff edge.

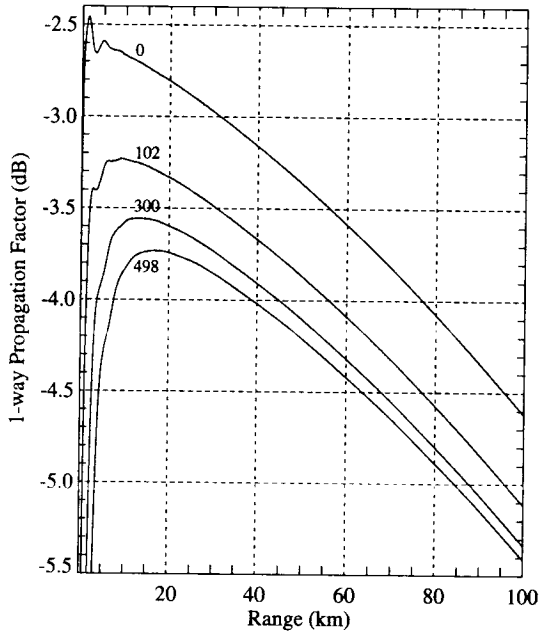

Fig. 4. Comparison of 3 MHz 1-way propagation factor calculated for four different cliff heights. The propagation path is 6 m above the sea surface. The curves are labeled with the cliff height specified in meters.

m and then slopes linearly down to a height of 0 m above sea level at a range of 110 m. The sea is smooth, and the refractivity structure corresponds to the standard atmosphere.

The TERPEM calculations are performed on a two dimensional grid spanning the range and height directions. Input parameters are required for the maximum range and height of the calculations, as well as the distances between adjacent range and height grid points. The upgraded TERPEM allows one million grid points to be shared between the height and range dimensions, with a limit of 50 000 grid points for the range direction. The range grid increment for the HF cliff calculations is chosen to be 10 m to allow the changes in terrain elevation to occur at a grid point. The height grid increment is 6 m.

The one-way propagation factor values calculated for cliff heights of 0, 102, 300, and 498 m are shown in Fig. 4. The 1-way propagation factor decreases as the cliff height is increased. However, at ranges far from the cliff (>10 km), the maximum decrease is less than 1 dB for cliffs having heights of up to 498 m. The trends of the plotted curves with range indicate that this decrease caused by the cliff will remain below 1 dB over the full operational range of HFSWR. Thus, cliffs having heights of up to 498 m do not significantly affect the propagation of the 3 MHz HFSWR signals.

V. Effective Ice Thickness

Broken sea ice is a common occurrence in the Arctic. Modeling of this type of terrain can easily be done within TERPEM by explicitly defining the properties (e.g., floe size, ice thickness) of each ice floe. However, a large number of grid points are required for explicit modeling of broken ice over large ranges.

It has been found through experience with TERPEM that obtaining consistent and correct results requires a range grid increment that is small enough such that all transitions between terrain types occur at a grid point and that each terrain segment contains at least 10 grid points. Given these constraints, even the upgraded TERPEM does not allow for enough grid points to explicitly describe the range dependence of the ice cover out to the maximum range of a HFSWR for some realistic cases of broken ice. For example, broken ice consisting of 90% ice coverage and a floe size of 20 m implies that the open water distances between ice floes is on average ~2 m. This would require a range grid increment of 0.2 m to allow for 10 grid points to be contained within the sea segments. This, in turn, would require two million range grid points to reach 400 km. Therefore, a different approach is required to model broken ice consisting of small floes.

It has been found that broken ice structures consisting of terrain segment sizes that are smaller than the radar wavelength can be effectively modeled with unbroken ice having an effective ice thickness t_e, given by the multiplication of the ice coverage fraction f_i, with the actual ice thickness t, i.e.

$$t_e = f_i t. \tag{1}$$

For example, for a broken ice structure of 60% fractional coverage consisting of 60 m floes having a thickness of 60 cm, the corresponding effective ice structure consists of solid ice (100% coverage) having a thickness of 0.6×60 cm $= 36$ cm. Fig. 5 shows a comparison of the propagation factor calculated for this case using both the explicit (small floes) and effective approaches. The geometry corresponding to the explicit approach is shown in Fig. 6. The terrain definitions for the explicit (small floes) and effective ice structures are given in Table I. Other relevant parameters are given in Table II.

In addition to the propagation factor data corresponding to the explicit representation of the small floes, Fig. 5 also shows equivalent data corresponding to explicit representations of medium floes (240 m), big floes (960 m), and vast floes (3840 m). In each case, the actual ice thickness is 60 cm and the open water distances between floes (medium: 160 m; big: 640 m; vast: 2560 m) are such that the total ice coverage is 60%. Thus, the propagation factor that would be calculated for each floe size using an effective ice thickness is the same as that shown for the small floes (solid black line). Hence, the comparison in Fig. 5 shows that the effective ice surface representation provides propagation factor data that agrees well

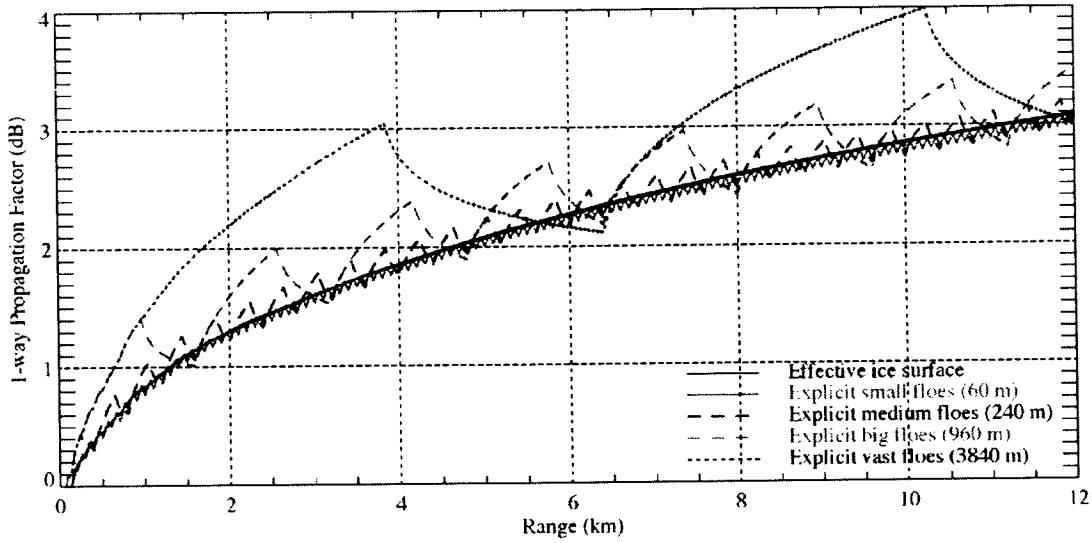

Fig. 5. Comparison of 3 MHz 1-way propagation factor over explicit and effective terrain definitions for a simple broken ice structure. The propagation path is 10 m above the sea or ice surface. The range grid increment is 4 m for all cases.

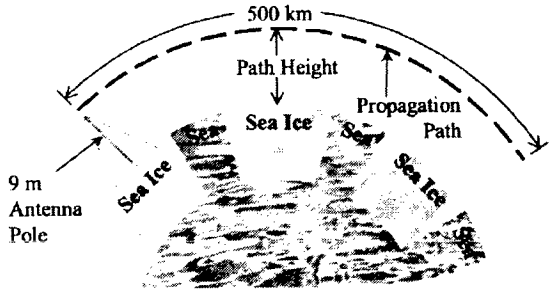

Fig. 6. Geometry for propagation calculations over seas covered with broken ice.

TABLE I
EXPLICIT AND EFFECTIVE TERRAIN DEFINITION FOR AN EXAMPLE BROKEN ICE CASE. IN THIS CASE, SEA ICE IS DEFINED BY $\varepsilon_r = 8, \sigma = 0.0011$ S m^{-1}, AND SEA IS DEFINED BY $\varepsilon_r = 70, \sigma = 2.55$ S m^{-1}

EXPLICIT DEFINITION

Starting Range (m)	*Upper Terrain Type*	*Upper Terrain Thickness (cm)*	*Lower Terrain Type*	*Lower Terrain Thickness (cm)*
0	Sea Ice	60	Sea	∞
60	Sea	∞	N/A	N/A
100	Sea Ice	60	Sea	∞
160	Sea	0	N/A	N/A
200	Sea Ice	60	Sea	∞
260	Sea	0	N/A	N/A
⋮	⋮	⋮		
39900	Sea Ice	60	Sea	∞
39960	Sea	0	N/A	N/A

EFFECTIVE DEFINITION

Starting Range (m)	*Upper Terrain Type*	*Upper Terrain Thickness (cm)*	*Lower Terrain Type*	*Lower Terrain Thickness (cm)*
0	Sea Ice	36	Sea	∞

TABLE II
TERPEM PARAMETERS FOR BROKEN ICE SCENARIO

PARAMETER	VALUE
Antenna type	Vertical centre-fed linear antenna (see Jackson [11])
Frequency	3 MHz
Antenna Height	Effective source point at 0 m
Refractivity structure	Standard atmosphere (4/3 earth)
Sea state	0
Range grid increment	4 m
Height grid increment	1 m

with that corresponding to explicit calculations only in the case of the small floes, i.e., in the case of terrain segment sizes that are less than the radar wavelength.

Natural occurrences of broken ice have more complicated range structures than the simple cases considered in Fig. 5. An example of a broken ice case consisting of small floes is that corresponding to code R of the June 1, 2001 weekly ice chart created by the Canadian Ice Service (see Fig. 7). This egg chart is implemented in TERPEM using the interpretation listed in Table III. The top line of the egg chart specifies the total concentration of ice in the designated area. The second line provides the partial concentrations for each of the ice types (age, thickness) coded in the third line. The fourth line specifies the floe size for each type. A detailed description of the egg chart codes is provided by the Canadian Ice Service [12]. For all calculations of this paper, total concentrations coded as 9+ (or 10) are interpreted as 100% ice coverage. Ice thickness is interpreted to be the mean of the coded range, or 160 cm in the case of thick first year ice, and 200 cm in the case of multiyear ice.

A specific realization of a broken ice structure, which can be used within TERPEM, is created as a series of floes with randomly generated sizes that are constrained within the size range specified by the egg chart. When the floe size range is unknown

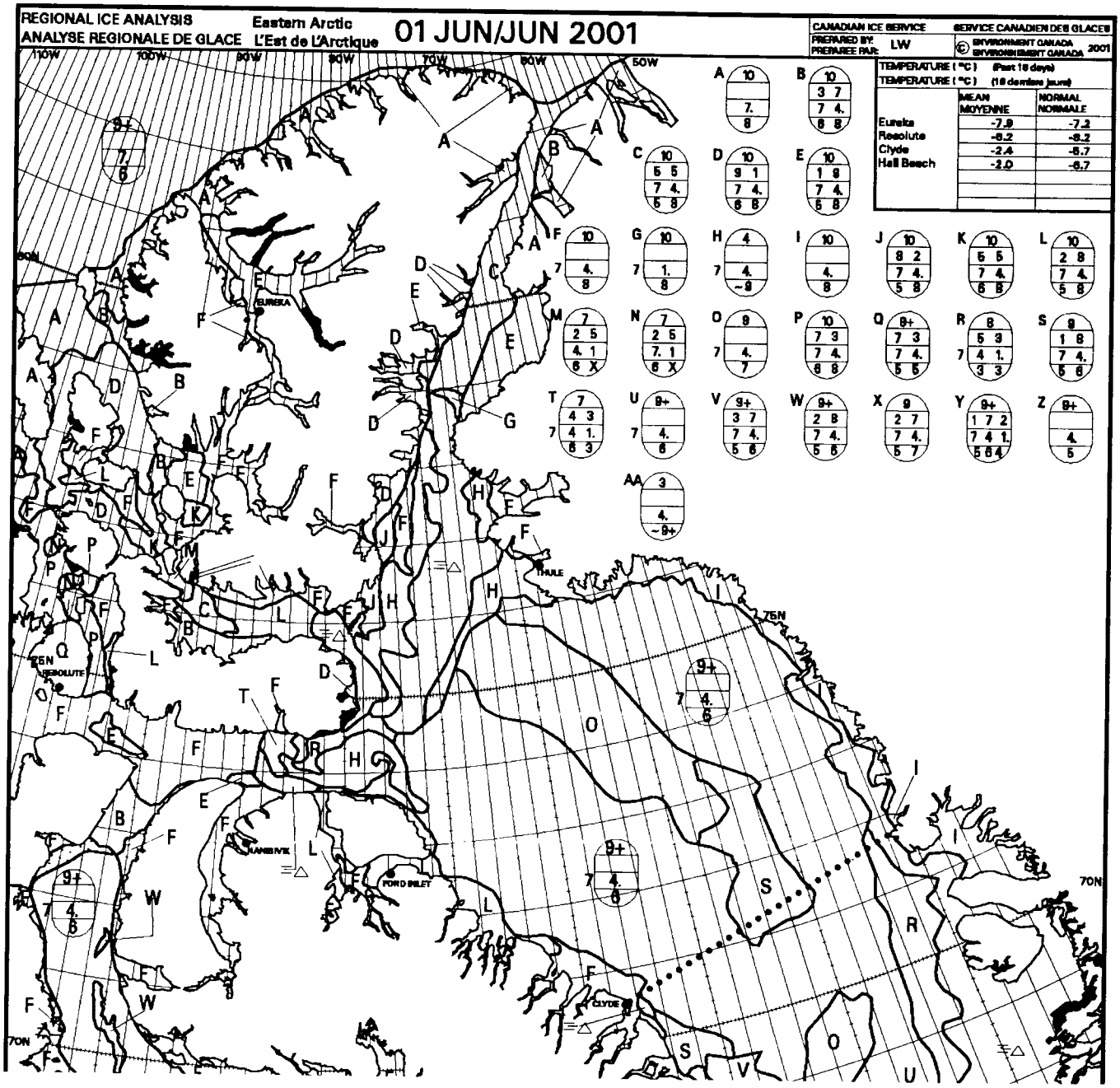

Fig. 7. Weekly ice chart issued on June 1, 2001 by the Canadian Ice Service for the Eastern Arctic region. The dotted line shows the propagation path used for site-specific calculations. The propagation path begins near Clyde River on Baffin Island and ends on the other side of Baffin Bay at Greenland.

TABLE III
REPRESENTATION OF CODE R EGG CHART (JUNE 1, 2001 EASTERN ARCTIC WEEKLY ICE CHART) FOR TERPEM CALCULATIONS

EGG CHART	FRACTIONAL ICE COVERAGE (%)	ICE THICKNESS (cm)	FLOE SIZE (m)
8 / 5 3 / 4 1. / 3 3	50	12.5	20-100
	30	95	20-100

(code X), the range given for an adjacent ice region is used. If the fractional ice coverage is less than 100%, then the open water lengths are chosen such that the distance between each ice floe is the same. The overall random structure must be created such that the open water distance between floes is also at least ten times the range grid increment. In addition, all contiguous regions of floes having the same ice thickness, including the open water between these floes, must have a length that is at least ten times the range grid increment. Once these constraints are satisfied, all regions that have floes smaller than the radar wavelength, and which contain open water, are converted into a single floe of effective ice thickness.

As an example, the propagation path (dotted line in Fig. 7) for the site-specific calculations discussed later requires the broken ice structure described in Table III to be realized over a range of 22 km. This is done by first generating a series of random floe sizes between 20 and 100 m. Each of these floes will be assigned

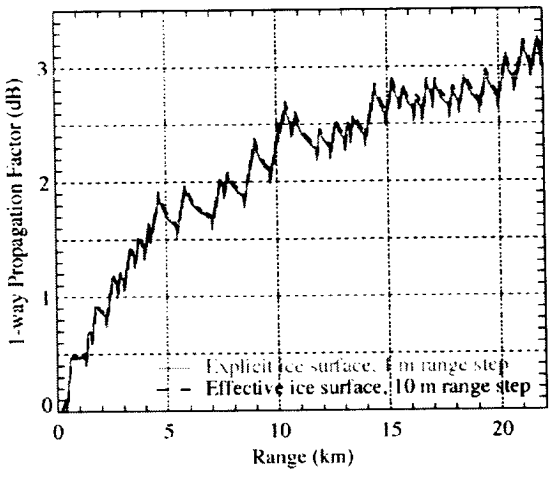

Fig. 8. Comparison of 3 MHz 1-way propagation factor over explicit and effective terrain definitions for a realistic broken ice structure. The propagation path is 10 m above the sea or ice surface.

an ice thickness of 12.5 cm. The total length of all these ice floes will equal 50% of the 22 km range (11 km). Then random floe sizes will be generated between 20 and 100 m and assigned an ice thickness of 95 cm. The total length of all of these floes will be 30% of 22 km (6.6 km). The remaining 20% of the 22 km (4.4 km) will be defined to be sea. The sea distances between floes will be set to 4.4 km divided by the total number of floes. The two different floe types (12.5 or 95 cm ice thickness) will be randomly mixed together over the 22 km range. However, if, for example, the range grid increment is chosen to be 10 m, then the mixing of the two ice types must be limited such that the length of any contiguous region of constant ice thickness, including the open water between floes, is at least 100 m.

For a 3 MHz radar, the floe sizes in the above example are smaller than the radar wavelength. Hence, all regions of contiguous ice thickness, and open water, will be converted to solid ice of effective ice thickness. Fig. 8 shows a comparison of propagation factor calculated by TERPEM for explicit and effective descriptions of this broken ice structure. The exact terrain definition used for the explicit calculations contains 285 sea segments and 285 sea-ice segments. The effective terrain definition contains 71 sea ice segments. The TERPEM parameters for this random case are the same as in the case of Fig. 5, except for the range grid increment, which is 1 m in the explicit case and 10 m in the effective case. The propagation factor curve corresponding to the effective ice thickness representation differs only very slightly from the case corresponding to the explicit representation. This type of agreement between explicit and effective ice thickness representations has been found for all test cases of randomly generated broken ice structures consisting of floes that are smaller than the radar wavelength. Thus, the approach of using effective ice thickness works well and greatly reduces the number of grid points required to complete the propagation calculations.

VI. Site-Specific Calculations

In simple cases, such as 100% coverage with sea ice, the presence of an ice layer generally causes the propagation factor near the surface to increase at short ranges and decrease at far ranges, relative to the all-sea case (see Thomson and Quach [4]). The

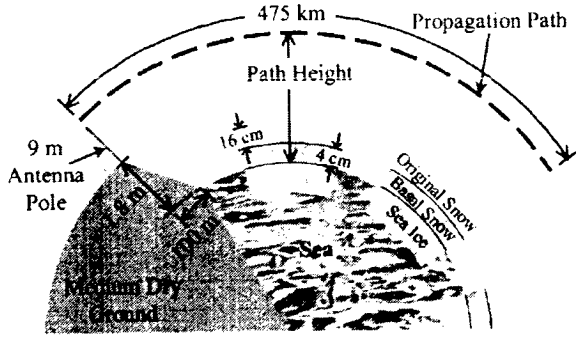

Fig. 9. Geometry for site-specific propagation calculations including broken sea ice and a snow layer.

range at which the propagation factor drops below that corresponding to the all-sea case is a function of the thickness of the ice layer. Thinner ice layers provide better improvement in propagation factor. For example, for the parameters listed in Table II (e.g., 3 MHz), the propagation factor at 10 m above the sea and at all ranges out to 500 km is larger for the case of 100% coverage with 30 cm of sea ice than it is for ice-free conditions (see Thomson and Quach [4]). However, for the case of 100% coverage with 2 m of sea ice, the propagation factor is significantly reduced at all ranges of interest. The results corresponding to more complicated and realistic ice structures display similar properties.

Site-specific calculations are performed for a propagation path that extends approximately 475 km from the Cape Christian Airfield, near Clyde River, Baffin Island, across Baffin Bay, to the Nunavik peninsula of Greenland (see dotted line in Fig. 7). This particular path was chosen since it is long enough to allow propagation effects to be studied over the full operational range of the HFSWR.

A range grid increment of 10 m is chosen for the calculations. Consequently, the requirement of 10 grid points per terrain segment demands that the minimum length of the modeled ground terrain is 100 m. Thus, for these calculations the antenna is chosen to be 100 m from the sea, where it will have an elevation of ~1.8 m (approximated from a topographical map). This elevation is very small compared to the radar wavelength of 100 m. Consequently, the terrain elevation is likely to have a negligible effect on these calculations. The terrain type between the antenna and the sea is assumed to be medium dry ground.

Random broken ice structures, corresponding to weekly ice charts issued by the Canadian Ice Service for nine different times during the year 2001, are modeled using the approach discussed above. The resulting structure corresponding to the January 1, 2001 ice chart, for example, contains a total of 238 terrain segments (see Thomson and Quach [4] for detailed information). The ice floes are covered with what is thought to be a typical snow layer, i.e., 4 cm of basal snow ($\sigma = 0.0332\ \mathrm{S\ m^{-1}}, \varepsilon_r = 2.4$, at 3 MHz, see Thomson and Quach [4] and Barber *et al.* [13]) and 16 cm of "original" snow ($\sigma = 6.73 \times 10^{-6}\ \mathrm{S\ m^{-1}}, \varepsilon_r = 1.82$, at 3 MHz, see Thomson and Quach [4] and Barber *et al.* [13]).

The geometry corresponding to the site-specific calculations is shown in Fig. 9. The height grid increment for the calculations is 5 m, and all other parameters, besides the grid increments, are as listed in Table II.

The one-way propagation factors corresponding to the nine cases, a radar frequency of 3 MHz, and a path height of 10 m,

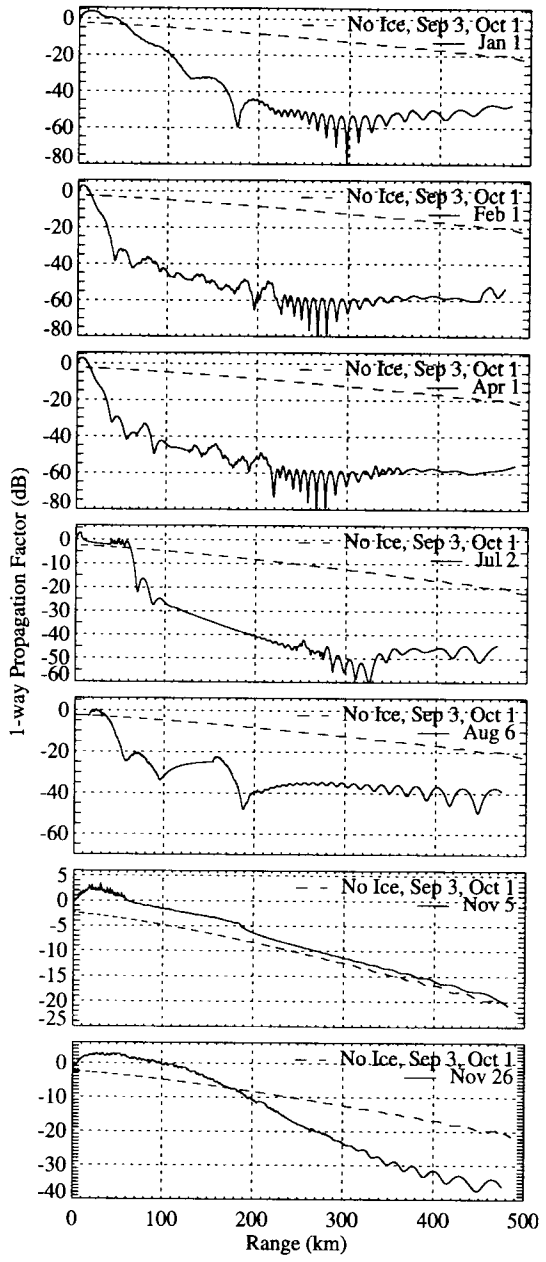

Fig. 10. Comparison of 3 MHz 1-way propagation factor over ice conditions corresponding to nine different times during the year 2001 with an additional snow layer. The propagation path is 10 m above the sea or ice surface, starting at the Cape Christian Airfield and ending at the Nunavik peninsula.

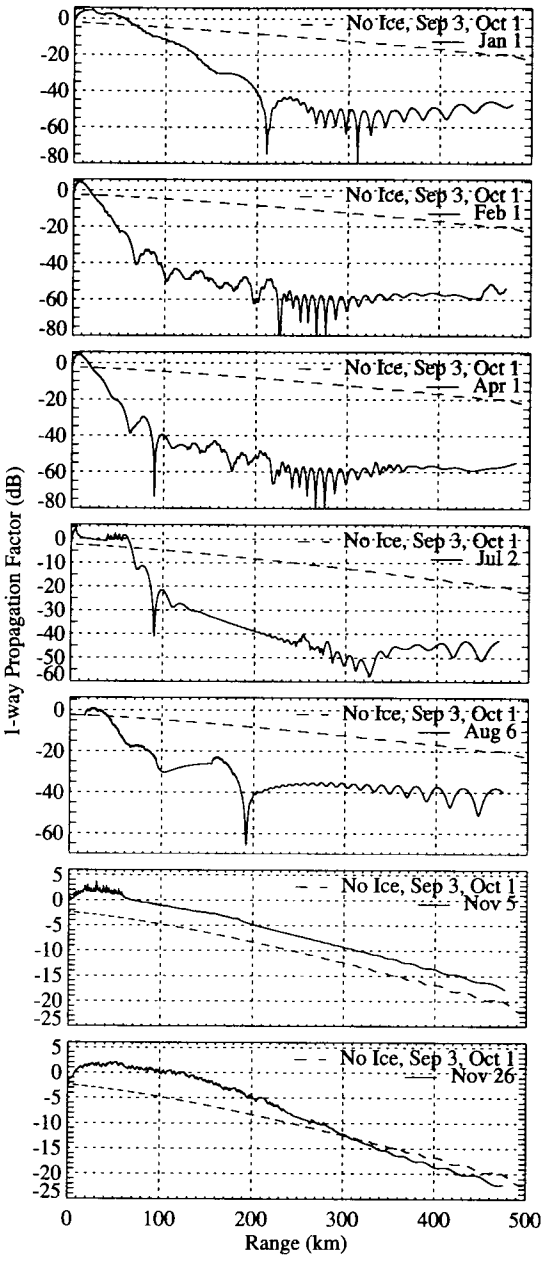

Fig. 11. Comparison of 3 MHz 1-way propagation factor over ice conditions corresponding to nine different times during the year 2001. The propagation path is 10 m above the sea or ice surface, starting at the Cape Christian Airfield and ending at the Nunavik peninsula.

are shown in Fig. 10 as a function of range. The ice conditions on September 3, 2001 and October 1, 2001 consisted of bergy water over the entire propagation path from Cape Christian to the Nunavik peninsula. Therefore, the terrain for these two dates was modeled as sea. Consequently, the HFSWR performance in arctic conditions, in terms of propagation, is assessed by comparing the calculated data with the data for these two dates. The results of similar calculations performed without the basal and "original" snow layers are shown in Fig. 11.

The data corresponding to all dates show an immediate drop in 1-way propagation factor of ~2.5 dB. This is caused by attenuation of the radar signal as it passes over the 100 m of medium dry ground between the antenna and the sea. Since this loss is common to all conditions, it does not affect the performance assessment determined by comparing the propagation data for ice conditions to that of the "no-ice" case.

Figs. 10 and 11, show that for the ice conditions of November 5, 2001, the propagation of the HFSWR signals is better than that for ice-free conditions along the entire path. In addition, the ice conditions of November 26, 2001 provide improved propagation, relative to the no-ice case, out to ~300 km for the case without snow and ~180 km for the case with snow. Thus, these data suggest that HFSWR performance at Cape Christian will be equal to or better than HFSWR performance for ice-free conditions over a significant range (~180 to 300 km) for a significant portion of the year (September to December). For the remainder of the year, the ice conditions greatly reduce the propagation of the HFSWR signals. However, the propagation is still better than

that for the no-ice case out to ~65 km range for the January 1, 2001 and July 2, 2001 ice conditions (no snow). In addition, a continued trend of increased warming in the Arctic will decrease ice thickness and hence increase the portion of the year for which the propagation corresponding to a HFSWR system located at the Cape Christian Airfield will be equal to or better than that corresponding to a system overlooking sea all year round.

VII. Summary and Conclusion

This paper examines HF (3 MHz) propagation over cliffs and in an arctic environment (e.g., broken sea ice, snow) using a modified version of the commercial software package TERPEM.

The results demonstrate that the TERPEM software is capable of producing very similar propagation results to those published by Hill and Wait [3] for the case of ice-covered seas. These results include both the "recovery effect," observed at sea/sea-ice terrain transitions, and the "interference effect" (see Hill and Wait [2], [3]). This agreement provides confidence in TERPEM since Hill and Wait [2], [3] used a completely different approach for their calculations ("residue series"). The main advantage of the parabolic equation methods used in TERPEM is that it easily allows the modeling of complicated, range-varying terrain structures. The modeling of such structures is necessary for propagation calculations in realistic arctic conditions.

The results corresponding to antennas located on cliffs demonstrate that cliffs up to 498 m, or ~5 wavelengths high, do not significantly affect the propagation of the HF signals. Therefore, in terms of propagation losses, these results suggest that it should be feasible to operate HFSWR systems from cliff tops.

It is also demonstrated that the propagation factors calculated by TERPEM over a broken ice structure, consisting of terrain segments that are smaller in length than the radar wavelength, are equivalent to the propagation factors calculated over a solid ice surface having a thickness equal to the actual thickness of each ice floe multiplied by the fractional ice coverage. Due to the limited number of range-height grid points available within TERPEM, the use of effective ice thickness within the greater terrain definition of a realistic sea-ice terrain is necessary to enable TERPEM to perform calculations out to the maximum operational range of the HFSWR.

Site-specific calculations out to 475 km range show that recent (year 2001) ice conditions in Baffin Bay would allow HFSWR propagation along the path from Cape Christian to the Nunavik peninsula of Greenland to be equal to or better than that in ice-free conditions out to a significant range for a significant portion of the year (~3 to 4 months), even with the presence of a snow layer.

The main conclusion of this report is that operation of HFSWR at selected locations in the Arctic should be feasible, at least for a significant portion of the year. This conclusion is based primarily on the comparison of theoretical propagation calculations in arctic conditions (cold, low-salinity water covered by sea-ice) with that over sea-only conditions. These calculations need to be confirmed through an experimental program. However, other aspects of HFSWR operation beyond propagation may also improve in the arctic environment. For example, the presence of sea ice will likely only dampen the amplitude of ocean waves and hence reduce the amount of sea clutter that can interfere with the detection of targets. In addition, ionospheric clutter affects HFSWR measurements at long ranges. Thus, for shorter-range surveillance problems, such as in the choke points of the Northwest Passage, ionospheric clutter should not be a problem. Man-made interference should also be less in the arctic environment, relative to that at mid-latitudes, simply because of the much smaller level of human activity. Finally, if the arctic climate undergoes significant warming in the near future then the thickness of sea-ice should decrease allowing for better HFSWR propagation.

References

[1] H. C. Chan, Long Range ship detection using high frequency surface wave radar, Defence Research Establishment Ottawa, DREO R 1184 1993.

[2] A. D. Hill and J. R. Wait, "HF radio wave transmission over sea ice and remote sensing possibilities," *IEEE Trans. Geosci. Remote Sensing*, vol. GE-19, no. 4, pp. 204–209, 1981.

[3] ——, "HF ground wave propagation over mixed land, sea, and sea-ice paths," *IEEE Trans. Geosci. Remote Sensing*, vol. GE-19, no. 4, pp. 210–216, 1981.

[4] A. D. Thomson and T. Quach, High frequency surface wave radar propagation in the Arctic, Defence R&D Canada—Ottawa, TR 2004-002 2004.

[5] M. F. Levy and K. H. Craig, HF Extension of TERPEM, (DREO CR 2001-121) (DREO, PWGSC Contract no. W7714-010484/A-GBL), Signal Science Limited, 2001.

[6] *TERPEM User Guide*, Signal Science Limited, 20 Alexander Close, Abingdon, Oxon, OX13 1XA, U.K., 1998.

[7] J. R. Wait, *Electromagnetic Waves in Stratified Media*. New York: Pergamon, 1962, p. 372.

[8] M. Levy, *Parabolic Equation Methods for Electromagnetic Wave Propagation*. London, U.K.: The Institution of Electrical Engineers, 2000, p. 336.

[9] L. V. Blake, *Radar Range-Performance Analysis*, Norwood, MA: Artech House, 1986, p. 443.

[10] E. C. Jordan and K. G. Balmain, *Electromagnetic Waves and Radiating Systems*, 2nd ed, NJ: Prentice-Hall, 1968, p. 753.

[11] J. D. Jackson, *Classical Electrodynamics*. New York: Wiley, 1962, p. 641.

[12] Environment Canada/Canadian Ice Service, Fact Sheet/Sea Ice Symbols,. *http://www.ice-glaces.ec.gc.ca/content_contenu/sea_ice_symbols_Jan2004.pdf?LnId=77* [Online]

[13] D. G. Barber, S. P. Reddan, and E. F. LeDrew, "Statistical characterization of the geophysical and electrical properties of snow on landfast first-year sea ice," *J. Geophys. Res.*, vol. 100, no. C2, pp. 2673–2686, 1995.

Alan D. Thomson received the B.Sc degree in physics from the University of Waterloo, Waterloo, ON, Canada, in 1990, and the M.Sc. and Ph.D. degrees in physics (cloud physics/radar meteorology) from the University of Toronto, Toronto, ON, Canada, in 1991 and 1996, respectively.

Since 1997, he has been employed as a Scientist by Defence Research & Development Canada—Ottawa. His current research interests include radar clutter and propagation in coastal regions, radar system and environment modeling, and related target detection problems.

Tan D. Quach received the B.A.Sc. degree in electrical engineering from the University of Ottawa, Ottawa, ON, Canada, in 2002, where he is currently working toward the M.A.Sc. degree in electrical engineering.

He has previously worked on microstrip antennas with the Advanced Antenna Technology Laboratory, Communications Research Centre, Ottawa, ON, Canada, and also on the propagation of HF signals in arctic conditions with Defence Research & Development Canada—Ottawa. His current research interests include antennas and computational electromagnetics.